Simulation and experiments for a broadband terahertz absorber

Dainan Zhang (张岱南)[1], Qiye Wen (文岐业)[2*], and Yunsong Xie (谢云松)[2]

[1]*Elite College, University of Electronic Science and Technology of China, Chengdu 610054, China*

[2]*State Key Laboratory of Electronic Films and Integrated Devices,*

University of Electronic Science and Technology of China, Chengdu 610054, China

**Corresponding author: qywen@163.com*

Received December 12, 2010; accepted January 11, 2011; posted online June 27, 2011

A metamaterial (MM) absorber is very attractive in the terahertz (THz) regime for its potential applications as a bolometer and thermal emitter. In this letter, we propose a transmission line model for the MM absorber in order to identify the basic absorption mechanism involved. Some strategies are put forward to widen the absorption bands to over 250 GHz. A new kind of MM absorber is designed, fabricated, and measured. The results show that a strong absorption of over 90% with a bandwidth of over 300 GHz is obtained, facilitating wide-frequency applications.

OCIS codes: 0300.6495, 300.1030.

doi: 10.3788/COL201109.S10402.

A metamaterial (MM) absorber is generally a three-layer structure with each layer significantly smaller than the wavelength[1]. These three layers are an electric split-ring resonator (eSRR) layer, a metal wire or plate layer, and a dielectric layer between them. The theoretical results show that a MM absorber can almost completely absorb the electromagnetic (EM) wave in a specific frequency band, thereby makes it an ideal candidate for bolometric pixel elements. The terahertz (THz) wave has attracted much attention for its potential applications, such as in THz imaging[2,3]. A MM absorber is especially attractive in the THz regime for its potential applications, thus it has received substantial research interest in recent years as a novel material[4−7]. However, the mechanism of near-unity absorption remains to be poorly understood to date. In this letter, based on our previous works[8−11], some interesting theoretical and experimental phenomena of this novel device are summarized and discussed in detail. We give an introduction to the proposed transmission line (TL) model for the metamaterial absorber (MA), and we examine the basic mechanism for EM absorption. From the TL model, two strategies are put forward to achieve broadband absorption at the THz regime. As an example, a new kind of MA is designed and fabricated. Both theoretical and experimental results confirm a strong absorption of over 90% with a bandwidth of over 300 GHz.

The first proposed MA aimed to obtain near-unity absorption[1], and some subsequent designs extended the properties of the absorber to be polarization insensitive, flexible, or wide in angle[4−7]. Regardless of function, however, the basic device structure generally includes two metallic elements: an eSRR layer and a background metal layer (BML). These two metal components are separated by a dielectric spacer. Actually, each metallic layer with its underlayer composes a MM. Therefore, the MA can be regarded as a composite of two different MMs separated by a functional material layer, and so it can be modeled by a TL model[9,10]. In this letter, we take two basic structures as examples to investigate the validity of the TL model, as shown in Fig. 1.

In the TL model, the transverse EM wave is assumed to propagate through free space and the substrate. There are two assumptions for constructing the TL model. Firstly, the coupling capacitor or coupling inductor between the eSRR layer and the wire layer should be ignorable so that these two layers can be individually modeled, as shown in Fig. 2. Secondly, the THz wave normally incidents into the absorber plane with the electrical field parallel to the split gap of the eSRR. The parameters R_1, L_1, and C_1 and R_2, L_2, and C_2 correspond to the LC and dipole resonance of the eSRR, respectively, and M refers to the coupling between them. R_3, L_3, and C_3 specify the resonance of the wire structure; TL refers to the transmission line which represents the separation layer; Z_i and Z_o are the input and output impedance of the system, respectively. All parameters need to be optimized until the S-parameters calculated by the TL model fit the simulation results. The detailed method for this can be found in our previous work[9,10].

With the TL model, we can arrive at some vital conclusions on the basic function of each component of the MA. (i) As hinted by the TL model, the LC resonance of the eSRR strongly affects the absorption characteristics of the absorber. Furthermore, for eSRR, the inductance L

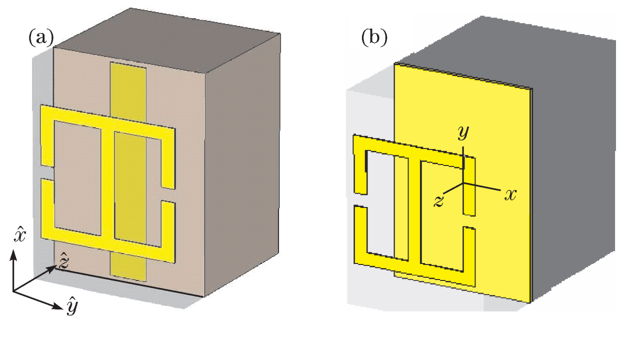

Fig. 1. Basic MA with a background metal layer of (a) wires and (b) plate.

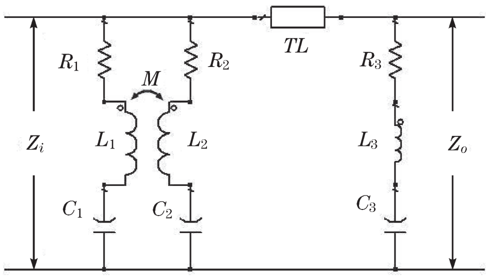

Fig. 2. TL model for MA.

is provided by its metallic loops, and the capacitance C is induced by the splits (cuts) of the ring. Thus, the absorption curve of the absorber mainly depends on the framework of the eSRR. (ii) More importantly, the function of the isolation layer is to adjust the impedance of the MM and to enable the EM wave to enter into the device as much as possible. Therefore, the absorption is highly sensitive to the properties of the isolation layer such as its thickness, permeability, and permittivity. (iii) The role of BML is to enhance the reflection of the EM wave, thereby benefiting the trapping and absorbing of wave in the space between the two metallic layers. Therefore, the replacement of the original wire structure by the metal plane producing a perfect absorption of over 99.9% is feasible[5]. In addition, further examination shows that the application of the metal plane brings much convenience in device design and fabrication. We should note that the absorption comes mainly from the dielectric loss of the isolation material or substrate. This indicates that the absorber can concentrate or trap the EM wave in some specific locations of the spacer or the substrate. Therefore, in these spots (for example, the space neighboring the split gap of the eSRR), the energy is significantly reinforced.

Narrow-band absorption is desired for some applications such as bolometric pixel elements. However, for many other applications such as the thermal emitter and invisible cloaking[12], wide-band absorption is also required in order to enhance device efficiency. We find that with the proposed TL model, identifying some design strategies to widen the absorption band is easy. One method is to increase the value of R_1 because the results from the TL model indicate that R_1 is responsible for most of the absorption. Another is to introduce several absorption bands and to combine them into a wide one. In the following, we present an illustration of how these problems can be solved by the TL model.

For the device design and fabrication, according to the discussion above, there are at least two ways to increase R_1. One is to lower the conductance of the material of eSRR (σ), similar to the frequency selective surfaces used in some microwave absorbers. Another way is to apply an isolation material with a large imaginary part of permittivity (ε"); the enhancement of leakage capacitance induces an increase in R_1. According to the TL model, the absorption enhancement in the former method is derived from the increase in ohmic loss of the eSRR metal, whereas in the latter, the absorption results from the dielectric loss of the spacer. We take the MA shown in Fig. 1(b) as an example for the two situations. By using a metal plane as BML, the transmission of the

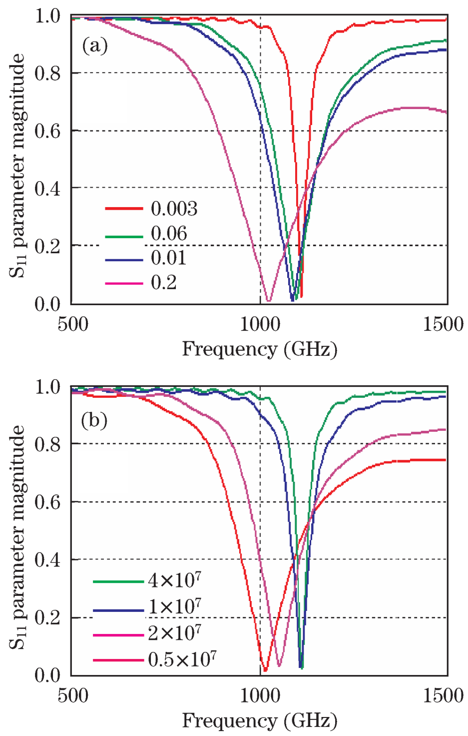

Fig. 3. Calculated S_{11} of the MA with different (a) imaginary parts of the permittivity of the spacer and (b) conductivities of the eSRR metal.

THz wave (S_{12}) through the absorber is zero. Therefore, the absorption can simply be calculated by $1-S_{11}^2$. The basic parameters are as follows: the metal used in the calculation is gold with σ of 4.09×10^7 S and thickness of 800 nm; the distance between the eSRR structure layer and BML is changed to obtain perfect absorption, and this space is filled with polyimide with ε=3.5+0.0105i, μ=1. the substrate material is a slice of GaAs with ε=12.9+0.0774i, μ=1.

By varying the values of ε" and σ, respectively, the S_{11} parameters of the absorber were calculated, as shown in Fig. 3. The full-width at half-maximum (FWHM) of the reflection S_{11} increases from 35 to 250 GHz as ε" increases from 0.003 to 0.2. Similarly, when the σ of the metal decreases from 4×10^7 S to 0.5×10^6 S, the FWHM of the reflection S_{11} increases from 35 to 200 GHz. In these calculations, the thickness of the polyimide spacer should increase from 7.5 to 20 μm in order to keep the impedance matched. For both cases, the resonance frequency exhibits a slight red-shift, which is reasonable because the impedance conduction is slightly changed.

Another method to widen the absorption peak is to combine several absorption peaks together. As indicated by the TL model, the absorption peak of the absorber under study is mainly determined by the LC resonance of the eSRR structure. Therefore, a specially designed eSRR structure with several overlapped LC resonances is expected to realize the wide-band absorption. As shown in the inset of Fig. 4, a complex eSRR structure is designed and integrated with a bottom metal plane to form an absorber. The device was fabricated on GaAs by sputtering Ti(40 nm)/Au(800 nm) followed by spin coating with a 10-μm polyimide. Another 200-nm Au film

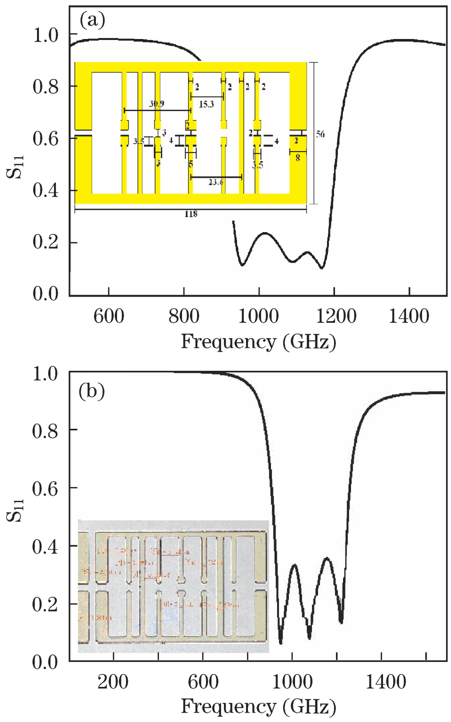

Fig. 4. S_{11} curves of the MA with broadband absorption. (a) Calculated results and (b) measured results. Insets in (a) and (b) are the schematic and SEM image of the absorber, respectively.

was sputtering deposited on the top of the polyimide film, which was then patterned into the designed eSRR shape by reactive ion etching. The dimension of the fabricated eSRR structure is marked in the photograph of a unit cell of the fabricated absorber.

Figure 4 shows the theoretical and experimental reflections of the MA. The simulation curve was calculated by using the TL model with a gold conductivity of 4.09×10^7 S and a polyimide dielectric constant of ε=3.5+0.0105i. Figure 4(b) shows the measured reflection by the THz time-domain-spectroscopy system, and the experimental details were described in Ref. [8]. There are three distinctive reflection peaks in both theoretical and experimental curves. These peaks are partly overlapped, giving rise to a bandwidth of 300 GHz at 90% absorption ($1-S_{11}^2$). This wide absorption at the THz band has never been reported previously.

Combining both methods, the wide-band absorption can easily be obtained. This wide-band feature of the MA facilitates its potential applications. For example, the MA may be an ideal candidate for use in solar cells if its dimension size scales down to the optical band. By replacing the current anti-reflection coating with the MA in solar cells[13], the interfacial reflection is reduced, and so more light is trapped. More importantly, by precise designing, the light can be concentrated and reinforced around the P-N junction, thereby significantly increasing the photoelectric conversion efficiency. Using the same principle, the absorber can also be integrated with thermal-electric materials to form a solar-thermal-electric system. When the solar energy is absorbed, in some specific spots, the temperature increases rapidly; in other places, however, the temperature is low, giving rise to a temperature difference for the thermal-electric effect.

In conclusion, we introduce a TL model for the MA, and the structure and basic physics mechanism have been discussed. We propose two kinds of methods to widen the bandwidth of the absorption. A new kind of MA is designed and fabricated, and a strong absorption over 90% with a bandwidth of over 300 GHz is obtained, paving the way toward the development of a wide-frequency THz absorber.

This work was supported by the National "973" Program of China (No. 2007CB310407) and the National Natural Science Foundation of China (Nos. 60801023 and 60721001).

References

1. N. I. Landy, S. Sajuyigbe, J. J. Mock, D. R. Smith, and W. J. Padilla, Phys. Rev. Lett. **100,** 207402 (2008).
2. J. Yang, S. Ruan, and M. Zhang, Chin. Opt. Lett. **6,** 29 (2008).
3. K. Yang, G. Zhao, C. Liang, and L. Wu, Chinese J. Lasers (in Chinese) **36,** 2853 (2009).
4. H. Tao, N. I. Landy, C. M. Bingham, X. zhang, R. D. Averitt, and W. J. Padilla, Opt. Express **16,** 7181 (2008).
5. H. Tao, C. M. Bingham, A. C. Strikwerda, D. Pilon, D. Shrekenhamer, N. I. Landy, K. Fan, X. Zhang, W. J. Padilla, and R. D. Averitt, Phys. Rev. B **78,** 241103(R) (2008).
6. Y. Avitzour, Y. A. Urzhumov, and G. Shvets, Phys. Rev. B **79,** 045131 (2009).
7. N. I. Landy, C. M. Bingham, T. Tyler, N. Jokerst, D. R. Smith, and W. J. Padilla, Phys. Rev. B **79,** 125104 (2009).
8. Q. Wen, H. Zhang, Y. Xie, Q. Yang, and Y. Liu, Appl. Phys. Lett. **95,** 241111 (2009).
9. Q. Wen, Y. Xie, H. Zhang, Q. Yang, Y. Li, and Y. Liu, Opt. Express **17,** 20256 (2009).
10. Q. Wen, H. Zhang, Y. Xie, Q. Yang, Y. Li, Chinese J. Opt. Appl. Opt. **3,** 70 (2010).
11. Q. Wen, Y. Xie, H. Zhang, Q. Yang, and Y. Li, Liu, Chinese J. Opt. Appl. Opt. **3,** 79 (2010).
12. D. Bouhafs, A. Moussi, A. Chikouche, and J. M. Ruiz, Sol. Energ. Mat. Sol. C **52,** 79 (1998).
13. D. Schurig, J. J. Mock, J. B. Justice, S. A. Cummer, J. B. Pendry, A. F. Starr, and D. R. Smith, Science **314,** 977 (2006).